Journal of Biomolecular NMR (2005) 31: 87–95

A protein backbone ψ and ϕ angle dependence of $^{2}J_{N(i),C\alpha(i-1)}$: The new NMR experiment and quantum chemical calculations

Wiktor Koźmiński[a,*], Igor Zhukov[b], Magdalena Pecul[a] & Joanna Sadlej[a]
[a]*Department of Chemistry, Warsaw University, ul. Pasteura 1, 02-093 Warszawa, Poland;* [b]*Institute of Biochemistry and Biophysics, Polish Academy of Sciences, ul. Pawińskiego 5a, 02-106 Warszawa, Poland*

Received 10 July 2004; Accepted 29 November 2004

Key words: coupling constants, DFT, *HNCO,* multiple quantum evolution, reduced dimensionality, theoretical calculations, ubiquitin

Abstract

A new pulse sequence exploiting double- and zero-quantum evolution of two-spin ^{15}N–$^{13}C'$ coherence is proposed for the accurate measurements of $^{2}J_{N(i),C\alpha(i-1)}$ coupling constants. Application of the new experiment is presented for ^{13}C,^{15}N-labeled ubiquitin sample. The density functional theory calculations of $^{2}J_{N(i),C\alpha(i-1)}$ coupling constants have been performed to study their dependence on both $\psi(i-1)$ and $\phi(i-1)$ angle in model peptides, and the results exhibit a good correlation with experimental data.

Introduction

Over the years, analysis of the torsion angles on the basis of the ^{3}J coupling constants and the Karplus relation (Karplus, 1963) has been widely used for determination of local conformation of proteins backbone (Bystrov, 1976). After introduction of residual dipolar couplings (RDC) as additional valuable constraints in determination of protein structure from NMR data (Tolman et al., 1995; Tjandra and Bax, 1997) the interest in ^{1}J and ^{2}J scalar coupling constants as well as ^{1}D and ^{2}D dipolar coupling constants has rapidly increased. Recently, numerous methods have been proposed for accurate measurement of different ^{1}J and ^{2}J coupling constants. These include *J*-modulated HSQC for measurement of $^{1}J_{N(i),C\alpha(i)}$ and $^{2}J_{N(i),C\alpha(i-1)}$ (Wirmer and Schwalbe, 2002), which was extended to *J*-correlated [^{15}N-^{1}H]-TROSY-HNC experiment (Wienk et al., 2003). Another technique is a HNCO experiment with a spin-state-selection module, which was used for evaluation of $^{1}J_{C'(i-1),C\alpha(i-1)}$, $^{1}J_{N(i),C'(i-1)}$, $^{1}J_{N(i),C\alpha(i)}$, $^{2}J_{N(i),C\alpha(i-1)}$, $^{2}J_{HN(i),C\alpha(i)}$, $^{3}J_{HN(i),C\alpha(i-1)}$, and $^{1}J_{C\alpha(i-1),C\beta(i-1)}$ (Permi et al., 2000) with a possibility of TROSY optimization (Permi and Annila, 2000). More sophisticated HSQC-TOCSY-HSQC experiments utilizing either $S^{3}CT$ (Meissner et al., 1997) or IPAP (Ottiger et al., 1997) approaches were proposed for measurements of $^{1}J_{N(i),C\alpha(i)}$, and $^{2}J_{N(i),C\alpha(i-1)}$ coupling constants (Heikkinen et al., 2001). Very recently a new experiment for determination of $^{1}J_{H\alpha(i),C\alpha(i)}$ and, $^{1}J_{C\alpha(i-1)C'(i-1)}$ coupling constants on the base of IPAP HSQC using accordion principle (Bodenhausen and Ernst, 1981, 1982) has been reported (Ding and Gronenborn, 2004a), and extended for determination of $^{1}J_{N(i),C\alpha(i)}$, $^{2}J_{N(i)C\alpha(i-1)}$ (Ding and Gronenborn, 2004b).

Relation between the backbone ϕ and ψ torsion angles and the $^{1}J_{N(i),C\alpha(i)}$ and $^{2}J_{N(i)C\alpha(i-1)}$ scalar coupling couplings was noted previously by several authors experimentally (Delaglio et al., 1991; Wirmer and Schwalbe, 2002, Ding and Gronenborn, 2004b), and theoretically (Edison et al., 1994a, b). Moreover, the Karplus-type relation has been parametrized with respect to

*To whom correspondence should be addressed. E-mail: kozmin@chem.uw.edu.pl

experimental values of $^{1}J_{N(i),C\alpha(i)}$ (Wirmer and Schwalbe, 2002; Wienk et al., 2003) and $^{2}J_{N(i),C\alpha(i-1)}$ (Wirmer and Schwalbe, 2002; Wienk et al., 2003; Ding and Gronenborn, 2004b) coupling constants. The $^{2}J_{N(i)C\alpha(i-1)}$ can be used as a valuable indicator to identify secondary structure elements in folded proteins (Wirmer and Schwalbe, 2002; Ding and Gronenborn, 2004b). However, the determination of given geometrical parameters from coupling constants is a nontrivial task because numerous other factors, not only the ϕ and ψ torsion angles, influence the magnitude of the coupling constants.

In principle, theoretical calculations constitute a perfect tool for establishing the correlation of spectroscopic parameters with molecular structure because it is possible to model systems of interest in every conformation. However, until recently, *ab initio* calculation of coupling constants in biochemical interest was practically impossible. Nowadays, it has become feasible to calculate spin–spin coupling constants – at least their dominant Fermi contact contribution – in realistic models of biomolecules by means of the density functional theory (DFT), and there are many works employing this methodology (see Helgaker and Pecul, 2004 for the review).

In this report we describe new simple and robust method for accurate measurements of $^{2}J_{N(i),C\alpha(i-1)}$ coupling constant based on recently proposed, reduced dimensionality (RD) (Szyperski et al., 1993a, b; Brutscher et al., 1994, 1995), double quadrature (Koźmiński and Zhukov, 2003) MQ-*HNCO* experiment (Koźmiński and Zhukov, 2004), and exploiting advantages of MQ-evolution for the determination of coupling constants (Rexroth et al., 1995). This technique is designed for extracting coupling constants of interest from zero- and double-quantum spectra and is ideally suitable for automated measurement of $^{2}J_{N(i),C\alpha(i-1)}$. Additionally, it enables identification of secondary structure elements on early stages of NMR protein structure determination.

In addition to the NMR experiment, quantum chemical calculations have been performed for two simple models of polypeptide: Ace-Ala-N-Me and Ace-Ala-Ala-N-Me. The surfaces of the spin–spin coupling constants generated by the rotation about the C—C and C—N bonds have been obtained. The calculated results have been fitted into a simple equation, and the predictions have been compared with experimental data.

Results and discussion

Pulse sequence

The pulse sequence scheme for the proposed $^{13}C_{\alpha}$-coupled-MQ-*HNCO* experiment is depicted in Figure 1. It employs out-and-back coherence transfer with excitation and detection of H_N protons, and is characterized by a single t_1 double- and zero-quantum coherences evolution period. The sensitivity enhancement detection block (Palmer III et al., 1991; Kay et al., 1992; Sattler et al., 1995) introduces ^{15}N phase modulation in t_1, while $^{13}C'$ evolution causes amplitude modulations. The characteristic feature of the proposed experiment is replacement of polarization transfers in INEPT manner by nested HMQC building blocks (Kay et al., 1990). As it was shown in our previous communication (Koźmiński and Zhukov, 2004), pulse sequences designed in this way consist of fewer pulses, and they are made as short as possible. The t_1 period is placed at the central point of the sequence, and directly after it the evolution is refocused in such a way that the effective evolution time of transverse magnetization is either equal to t_1 for coherences of interest or equal to zero. The ^{13}C carrier offset was constant for the whole duration of pulse sequences and set to the center of $^{13}C'$ region (176 ppm). Since active coupling does not evolve for MQ-coherences, the $^{1}J_{N(i),C'(i-1)}$ couplings need not to be refocused in the t_1. The couplings involving passive spins, however, give rise to splittings- equal to sum and difference of coupling constants with $^{15}N_{(i)}$ and $^{13}C'_{(i-1)}$, in double- and zero-quantum spectra, respectively. Only splittings due to spin–spin coupling with $^{13}C_{\alpha(i-1)}$ could be resolved in a typical protein sample, owing to relatively large $^{1}J_{C'(i-1),C\alpha(i-1)}$, typically of in the range of 50–55 Hz. The splittings due to $^{1}J_{N(i),C\alpha(i)}$ combined with relatively small $^{2}J_{C'(i-1),C\alpha(i)}$ are not observable.

Neglecting, in the first approximation, cross-correlation effects and vanishing ^{13}C–^{15}N dipolar interaction, relaxation rate of DQ/ZQ coherences could be assumed as sum of respective single-quantum relaxation rates. Therefore, the obtain-

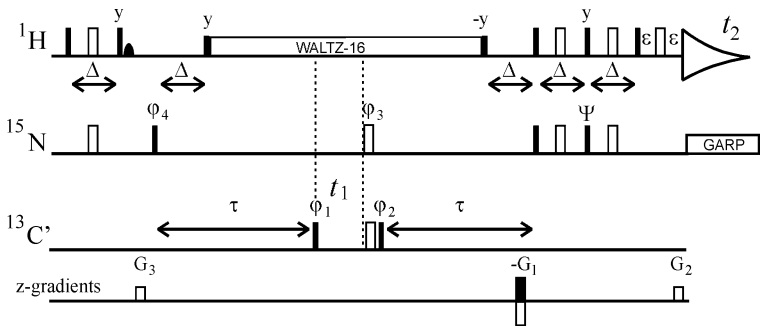

Figure 1. The pulse sequence of the reduced dimensionality DQ/ZQ 2D $^{13}C_{\alpha}$-coupled-*HNCO* experiment. Dark-filled and open bars represent $\pi/2$ and π pulses, respectively. The selective rectangular $^{13}C'$ pulses are applied on resonance with γB_1 set to $\Delta\Omega/\sqrt{15}$ and $\Delta\Omega/\sqrt{3}$ for $\pi/2$ and π pulses, respectively, where $\Delta\Omega$ is a difference between centers of $^{13}C'$ and $^{13}C_{\alpha}$ spectral regions. Water flip-back was applied as a sinc-shaped pulse of 2.1 ms duration, in the initial INEPT step. The ^{13}C carrier offset was set to the center of the $^{13}C'$ region (176 ppm). All pulses were applied along the rotating-frame x-axis unless indicated differently. The delay Δ should be tuned to $0.5/^1J(^{15}N, ^1H)$, and τ set to 28 ms for maximum amplitude of polarization transfer between ^1H, ^{15}N, and ^{13}C. ε includes the rectangular – shaped gradient pulse and a 100 μs recovery time. The basic phase cycle is: $\varphi_1 = x,-x$, $\varphi_2 = x,x,-x,-x$, $\varphi_3 = 8x,8y,8(-x)8(-y)$, $\varphi_4 = 4x,4(-x)$, and $\varphi_R = x,-x,-x,x,2(-x,x,x,-x),x,-x,-x,x$. ^{15}N quadrature was obtained using echo-anti-echo PFG-selection by G1 and G2 gradients with duration of 1 ms, and the relative amplitude of $\pm\gamma_H/\gamma_N$, with phase ψ set to $-y$ in echo, and $+y$ in antiecho experiments, respectively. $^{13}C'$ quadrature was obtained by $\pi/2$ phase shifts of $\varphi 1$ (States et al., 1982). The double quadrature detection requires acquisition of four data sets per each t_1. The axial peaks were displaced by simultaneous reversing of the sign of φ_1 and receiver phase (φ_R) for the even t_1 increments (Marion et al., 1989).

able resolution is decreased in comparison to methods with ^{15}N SQ-evolution. In the proposed experiment this causes vanishing of $^1J_{N(i),C\alpha(i)}$ splittings. However, the evolution of multiple quantum coherences is very useful for accurate measurements of coupling constants with passive spins. It is known that in the case when a relatively large coupling is combined as a sum or as a difference with a small one, the accuracy of the latter is improved due to weaker effects of differential relaxation (Abragam, 1961; Harbison, 1993). This outcome was for the first time explored for the measurement of $^3J_{HN,H\alpha}$ coupling constants in proteins (Rexroth et al., 1995). The systematical errors due to differential relaxation give rise to underestimated data, but their size is inversely proportional to the magnitude of splitting. Therefore since in proposed experiment $^2J_{N(i),C\alpha(i-1)}$ of magnitude 6–11 Hz is measured in combination with $^1J_{C'(i-1),C\alpha(i-1)}$ of ca. 55 Hz, the almost fivefold reduction of systematical errors is expected. The extraction of coupling data from DQ/ZQ spectra was also successfully applied in the field of organometallic chemistry (Otting et al., 1999).

Application of the double quadrature is essential for evaluation of single quantum frequencies, and enables separation of zero- and double-quantum spectra. It requires interleaved acquisition of an array of four data sets per each t_1 increment. The appropriate processing scheme has already been comprehensively described (Koźmiński and Zhukov, 2003). Here we only note that it relies on coaddition of a cosine and sine amplitude modulated data sets with $\pm\pi/2$ phase correction of the latter in t_1.

The double and zero-quantum spectra obtained using $^{13}C_{\alpha}$-coupled-MQ-*HNCO* sequence for sample of 1.5 mM ^{13}C, ^{15}N-labeled ubiquitin are shown in Figure 2a and b, respectively. The signal dispersion is enhanced by combination of both ^{15}N and $^{13}C'$ frequencies in the F_1 domain. In comparison with a conventional *HNCO* experiment the cross-peaks are split along F_1 dimension into doublets due to the sum and the difference of $^{15}N_{(i)}$ and $^{13}C'_{(i-1)}$ coupling with $^{13}C_{\alpha(i-1)}$, respectively. It is noteworthy that DQ/ZQ experiment preserves information about relative signs of coupling constants. The larger magnitude of splittings in apparent DQ-spectra (with multiplets centered at $\delta(^{13}C) + \delta(^{15}N)$, see Figures 2 and 3), with regard to the negative sign of $\gamma(^{15}N)$ (Levitt, 1997) enables us to attribute the negative sign to the measured $^2J_{N(i),C\alpha(i-1)}$ coupling constants. The negative sign of the $^2J_{N(i),C\alpha(i-1)}$ coupling, therefore the positive sign of the reduced $^2K_{N(i),C\alpha(i-1)}$ coupling, ($K_{AB} = 4\pi^2 h/\gamma_A\gamma_B \times J_{AB}$) is consistent with positive signs of other reduced geminal couplings

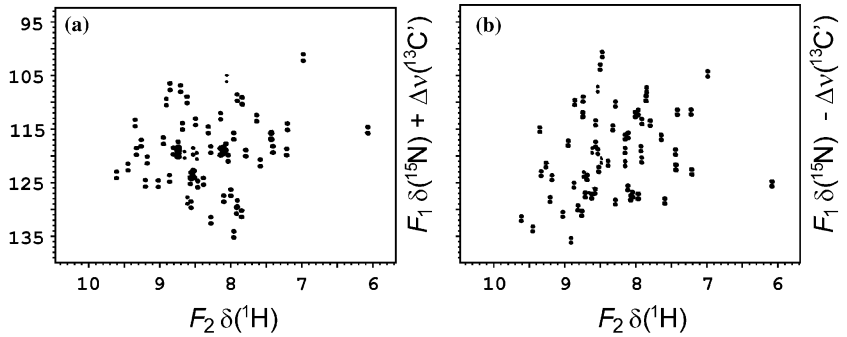

Figure 2. Contour plots of two-dimensional spectra obtained for ^{13}C, ^{15}N-labeled ubiquitin using the reduced dimensionality 2D $^{13}C_\alpha$-coupled-*HNCO* sequence from Figure 1. Plots (a) and (b) show double and zero quantum spectra, respectively. The time-domain data was processed, according to previously published procedure (Koźmiński and Zhukov, 2003) with retention of positive ^{15}N frequencies. The signal frequency in F_1 domain is equal to $\delta(^{15}N) \pm \Delta\nu(^{13}C')$, where $\Delta\nu(^{13}C')$ denotes frequency differences between $^{13}C'$ resonance and carrier offset. Thirty two scans were coherently added for each data set for 256 t_1 increments. The maximum t_1 and t_2 times were 85 and 82.6 ms, respectively. The spectral width of 3100 Hz, covering the sum of ^{15}N and $^{13}C'$ spectral ranges, was set for the F_1 dimension. A relaxation delay of 1.5 s was used. The data matrix containing 256 × 512 complex points in t_1 and t_2, respectively, was zero-filled to 8192 × 2048 complex points. Cosine square weighting function was applied prior to Fourier transformation in both dimensions.

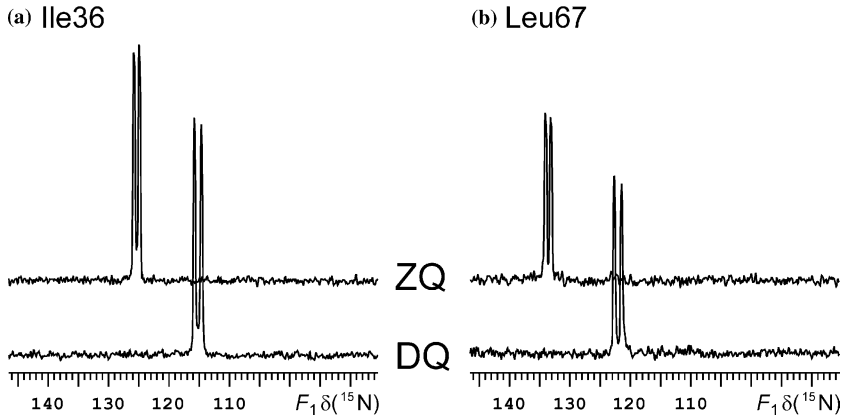

Figure 3. The F_1 cross sections across amide resonance of Ile36 (a) and Leu67 (b) taken from spectra presented in Figure 2. The signal frequencies in upper and lower traces represent DQ and ZQ spectra with difference and sum of the involved frequencies, respectively. The splittings are equal to sum and difference of $^1J_{C'\ (i-1),C\alpha(i-1)}$ and $^2J_{N(i),C\alpha(i-1))}$, in DQ and ZQ spectra, respectively. However to obtain correct sign of $^2J_{N(i),C\alpha(i-1)}$ the negative sign of $\gamma(^{15}N)$ should be considered (Levitt, 1997).

($^2K_{HH}$, $^2K_{CH}$) across the carbonyl group (see Contreras and Peralta, 2000; and experimental papers quoted therein).

Figure 3 provides two different examples of F_1 cross-sections through amide resonance of Ile36 (a) and Leu67 (b) obtained from the spectra presented in Figure 2. The distinctive features of the spectra are good resolution and high signal to noise ratio. The $^1J_{N(i),C\alpha(i)}$ splittings are not resolved.

The coupling constants were evaluated using peak-picking procedure of zero- and double-quantum spectra in Sparky program (Goddard and Kneller). We estimated, on the base of digital resolution and signal to noise ratio, the accuracy of experimental $^2J_{N(i),C\alpha(i-1)}$ coupling constants to ±0.3 Hz. It could be further improved by appropriate signal deconvolution. The $^2J_{N(i),C\alpha(i-1)}$ values are available in Supplementary Materials, and the obtained coupling data generally agree with previously published $^2J_{N(i),C\alpha(i-1)}$ coupling constants for ubiquitin (Heikkinen et al., 2001).

The new pulse sequence proposed in this work could be compared with the IPAP-type method proposed recently by Ding and Gronenborn (2004b), in which the relatively small $^1J_{N(i),C\alpha(i)}$

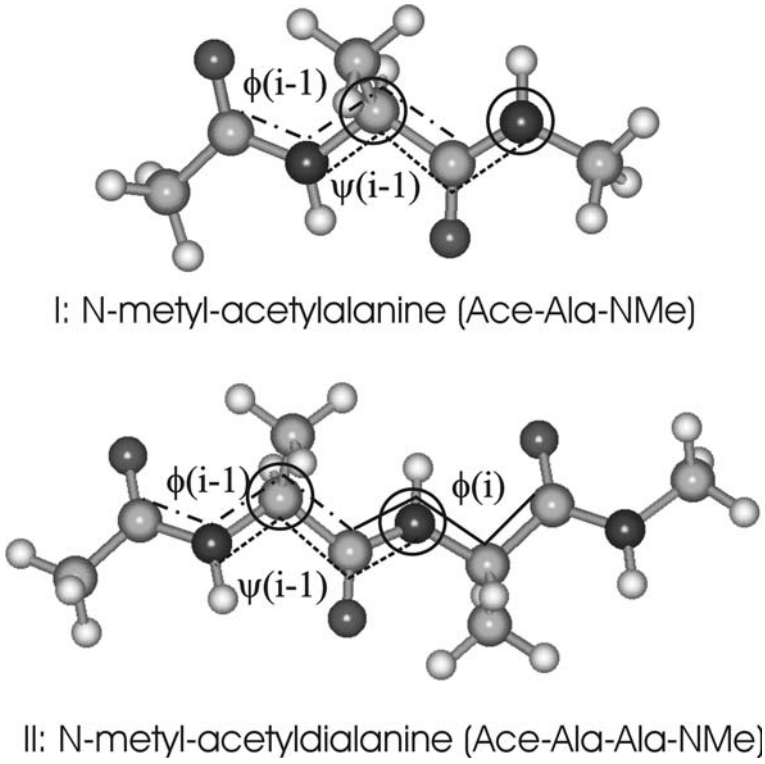

Figure 4. Structures of models Ace-Ala-N-Me and Ace-Ala-Ala-N-Me, with torsion angles $\phi(i-1)$, $\psi(i-1)$, and $\phi(i)$ marked. The coupled nuclei are marked by circles.

and $^2J_{N(i),C\alpha(i-1)}$ couplings evolve and give rise to small splittings. Therefore the latter method is more prone to systematic error due to differential relaxation and line-width effects, so it requires slow relaxation rates and excellent resolution.

All the spectra presented were recorded at 298 K on a Varian Unity Plus 500 spectrometer equipped with a Performa II z-PFG unit and a 5 mm ^1H, ^{13}C, ^{15}N-triple resonance probehead. High power ^1H and ^{15}N $\pi/2$ pulses of 6.5 and 48.0 μs, respectively, were employed. A sample of 1.5 mM ^{13}C,^{15}N-labeled ubiquitin in 9:1 H_2O/D_2O at pH = 6.0 was used. The experimental details are given in the Figure legends.

Calculations

The aim of the calculations was to correlate the $^2J_{N(i),C\alpha(i-1)}$ couplings in polypeptide with the backbone conformation. The first set of calculations was carried out on the model alanine dipeptide analogue, Ace-Ala-N-Me. The same peptide model has been previously used for modeling of the conformational dependence of $^1J_{C\alpha C\beta}$ (Cornilescu et al., 2000), proton chemical shift (Sitkoff and Case, 1997), and vibrationally averaged dipolar coupling strengths (Case, 1999). The torsion angles $\phi(i-1)$ and $\psi(i-1)$, shown in Figure 4, represent the rotation about the (N—C_α) and (C_α—C′) bonds, respectively. The $\phi(i-1)$ and $\psi(i-1)$ backbone torsion angles were sampled every 30° over the entire ϕ/ψ space. A set of these angles thus represents the conformation at the α-carbon atom. The second set of calculation was performed for a larger peptide model, Ace-Ala-Ala-N-Me, in order to investigate the dependence of $^2J_{N(i),C\alpha(i-1)}$ on the second torsion ϕ angle, denoted as $\phi(i)$ (see Figure 4).

The geometry optimization were carried out at the DFT-B3LYP (Becke-3-Lee-Yang-Parr) level as implemented in Gaussian 98 (Frisch et al., 1998) using the augmented correlation-consistent basis set aug-cc-pVDZ on N, C, O and cc-pVDZ on H (Dunning, 1989). The full geometry optimization have been performed for the

Ace-Ala-N-Me molecule with $\phi(i-1)$ and $\psi(i-1)$ angles frozen at their respective value from the grid. The indirect spin-spin coupling constants have been calculated at the DFT level using B3LYP functional (Becke, 1993; Stephens, 1994) as implemented in a local version of the DALTON program (Helgaker et al., 2001). We used the HII-su2 basis set (Schindler, 1982),which contains the tight s functions necessary for the spin–spin couplings calculations, on the coupled nuclei, and the HII basis set on the other nuclei. The spin-dipole (SD) term, the most time-consuming one, was omitted from the calculations, and only Fermi contact (found to dominate the conformational dependence of the coupling) and spin–orbit terms were included.

The calculated dependence of the $^2J_{N(i),C\alpha(i-1)}$ coupling on the $\phi(i-1)$ and $\psi(i-1)$ torsion angles in Ace-Ala-N-Me is shown in Figure 5. The minimal (in a sense of the absolute value) values of $^2J_{N(i),C\alpha(i-1)}$ (minimum −7.49 Hz) are for $\psi(i-1)$ in the range $-30 < \psi(i-1) < 30$ and for $\phi(i-1)$ close to 180°, while the maximum values of this spin–spin coupling (up to −13.61 Hz) are for $\psi(i-1)$ equal ca 120° and $\phi(i-1)$ close to 0°. When one compares this range with the experimental values of $^2J_{N(i),C\alpha(i-1)}$ couplings, they seem overestimated. However, it should be mentioned at this point that the range when the calculated absolute values of the couplings are the highest is also very high in the energy (approximately 70 kJ/mol above the global minimum), and such conformations are not assumed in nature. Other possible sources of error include: (a) strong electron correlation effects for the geminal coupling constants (and more so for the geminal couplings across the carbonyl carbon atom), difficult to render even by means of more sophisticated computational methods than DFT/B3LYP, although this method, while tending to overestimate the couplings (as in our case) is well suited for the calculations of the coupling constants to the proton, nitrogen and carbon (Pecul and Helgaker, 2003; Helgaker and Pecul, 2004); (b) the fact that the calculations were performed for a rigid molecule, without taking into account the vibrational effects; (c) possibly the basis set incompleteness, although the basis set employed should be suitable for the purpose; (d) incompleteness of the molecular model (see below).

The dependence of the coupling constants on the $\phi(i-1)$ and $\psi(i-1)$ backbone torsion angles calculated for Ace-Ala-N-Me was fitted to a truncated Fourier series, containing at most four terms, in a least-squares manner. Such a series has been used for fitting of the dependence of most of the calculated coupling constants on the dihedral angles on many occasions (Contreras et al., 2003). The resulting fitting equation is: $^2J_{N(i),C\alpha(i-1)} = -10.1982 - 1.2395\cos[\psi(i-1) - 140] - 0.4346\cos[2(\psi(i-1) - 140)] - 0.8644\cos[\phi(i-1)]$. Figure 6a contains the correlation

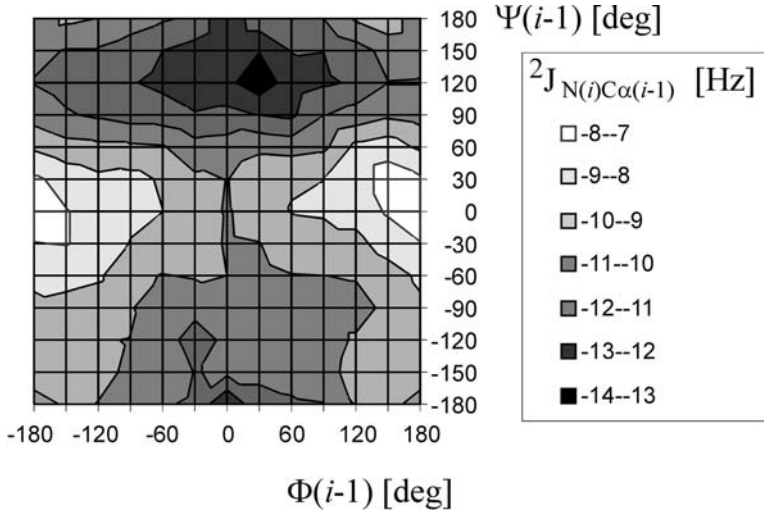

Figure 5. The dependence of the $^2J_{N(i),C\alpha(i-1))}$, coupling (in Hz) calculated for Ace-Ala-N-Me on the $\phi(i-1)$ and $\psi(i-1)$ torsion angles.

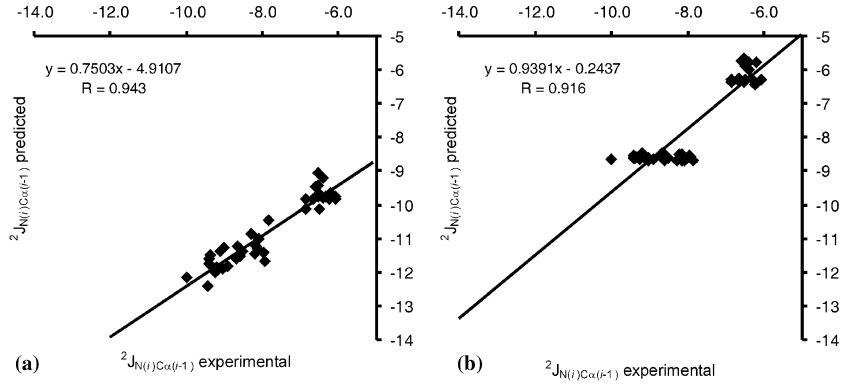

Figure 6. The correlation between experimental $^2J_{N(i),C\alpha(i-1)}$ coupling constants obtained for ubiquitin sample by application of pulse sequence from Figure 1, and their predicted values. (a) using the equation: $^2J_{N(i),C\alpha(i-1)} = -10.1982 - 1.2395\cos[\psi(i-1) - 140] - 0.4346\cos[2(\psi(i-1) - 140)] - 0.8644\cos[\phi(i-1)]$ obtained from calculations, and (b) using the empirical formula: $^2J_{N(i),C\alpha(i-1)} = -\{7.8509 - 1.5176\cos[\psi(i-1)] - 0.6616\cos^2[\psi(i-1)]\}$ (Ding and Gronenborn, 2004). Data calculated using ϕ and ψ torsion angles from structure of ubiquitin 1D3Z (Cornilescu et al., 1998) deposited in PDB databank (http://www.rcsb.org/pdb).

between the calculated and experimentally measured $^2J_{N(i),C\alpha(i-1)}$ couplings (each coupling compared for the given ϕ/ψ pair). As one can see, the correlation is not perfect. To some extent it can be attributed to the above mentioned overestimation of the couplings by DFT/B3LYP. The fact that the fit for the theoretical values was done for the entire space of ϕ/ψ, while in fact only a subset of it is probed by the protein also contributes. Another, and most probably even more substantial source of errors is not taking into account the dependence of $^2J_{N(i),C\alpha(i-1)}$ on the $\phi(i)$ torsion angle (see Figure 4). To check this hypothesis the dependence of $^2J_{N(i),C\alpha(i-1)}$ on $\phi(i)$ was investigated by means of the calculations of the Fermi contact term only for the extended model, Ace-Ala-Ala-N-Me, where $\phi(i-1)$ and $\psi(i-1)$ were fixed at the values of $-120°$ and 150°, respectively, and $\phi(i)$ was probed every 30°. The resulting dependence visualized in Figure 7 clearly shows that the dependence on $\phi(i)$, although smaller than on $\phi(i-1)$ and $\psi(i-1)$ (compare Figure 5) is not negligible (the changes of $^2J_{N(i),C\alpha(i-1)}$ span 2 Hz), and should not be ignored. Unfortunately, the rigorous probing of the entire $\phi(i-1)/\psi(i-1)/\phi(i)$ conformational space is not feasible at the moment (the calculations of the couplings alone, without geometry optimization, would take approximately 6.5 years of CPU time). Another possible source of error is the fact that the peptide CN bonds in the alanine dipeptide analogue optimized at the DFT level seem to long in comparison with the X-ray data. Setting them to the values of 1.33 Å causes a slight decrease in the calculated $^2J_{N(i),C\alpha(i-1)}$ coupling, but too small (0.1 Hz) to account for the discrepancy with experiment. However, it shows the sensitivity of this coupling to the quality of the molecular geometry.

Figure 6b shows the plot of correlation between the $^2J_{N(i),C\alpha(i-1)}$ couplings predicted by means of the empirical parametrization $^2J_{N(i),C\alpha(i-1)} = -\{7.8509 - 1.5176\cos[\psi(i-1)] - 0.6616\cos^2[\psi(i-1)]\}$ (Ding and Gronenborn, 2004b) and measured in the present work. The resulting slope and intercept of linear regression line are in this case correct. However, the two groups of points appear separately, which enables only a

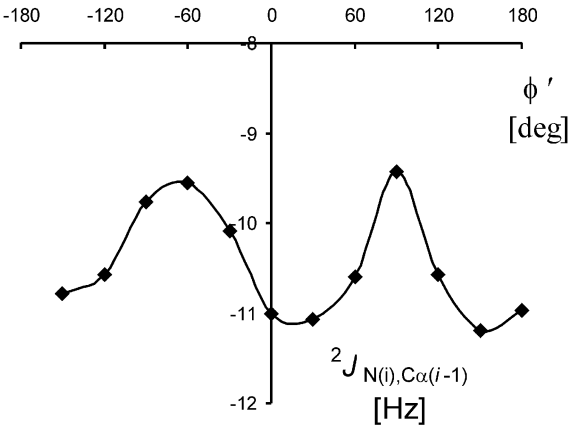

Figure 7. The dependence of the $^2J_{N(i),C\alpha(i-1)}$, coupling (in Hz) calculated for Ace-Ala-Ala-NMe on the $\phi(i)$ torsion angle, with $\phi(i-1)$ and $\psi(i-1)$ fixed at the values of -120 and 150°, respectively.

qualitative discrimination between secondary structure elements. Most probably there are two reasons of such behavior of empirically parametrized ϕ/ψ equation. First, the dependence of $^{2}J_{N(i),C\alpha(i-1)}$ on the $\phi(i-1)$ angle is ignored. Second, the experimental data span only a narrow regions of entire ϕ/ψ space. The other equation provided by Wirmer and Schwalbe (2002) is very similar to the above one, and is unlikely to change the conclusions.

Conclusions

We proposed a new technique for determination of $^{2}J_{N(i),C\alpha(i-1)}$ coupling constants based on $^{13}C_{\alpha}$-coupled double- and zero-quantum HNCO experiment. The experiment is sensitive and provides coupling data with significantly reduced influence of differential relaxation systematic errors. It could be applied for accurate determination of $^{2}J_{N(i),C\alpha(i-1)}$ and $^{1}J_{C'(i-1),C\alpha(i-1)}$ scalar, as well as $^{2}D_{N(i),C\alpha(i-1)}$ and $^{1}D_{C'\ (i-1),C\alpha(i-1)}$ residual dipolar couplings. The density function calculations of $^{2}J_{N(i),C\alpha(i-1)}$ show the ability of the DFT method for prediction of NMR parameters for biomolecules. The theoretical results correlate with the experimental data and can be used for their interpretation.

Acknowledgements

The authors are grateful to Prof Andrew R. Byrd (Structural Biophysics Laboratory, National Cancer Institute-Frederick, Frederick, Maryland, USA) for the sample of ^{13}C, ^{15}N-double labeled ubiquitin. M. P. thanks the Norwegian Research Council for computer time from the Supercomputing Programme.

Supplementary material to this paper is available in electronic form at http://dx.doi.org/10.1007/s10858-004-7563-7.

References

Abragam, A. (1961) *Principles of Nuclear Magnetism*, Clarendon Press, Oxford.

Becke, A.D. (1993) *J. Chem. Phys.*, **98**, 5648–5652.

Bodenhausen, G. and Ernst, R.R., (1981) *J. Magn. Reson.*, **45**, 367–373.

Bodenhausen, G. and Ernst, R.R. (1982) *J. Am. Chem. Soc.*, **104**, 1304–1309.

Brutscher, B., Cordier, F., Simorre, J.P., Caffrey, M.S. and Marion, D. (1995) *J. Biomol. NMR*, **5**, 202–206.

Brutscher, B., Simorre, J.P., Caffrey, M.S. and Marion, D. (1994) *J. Magn. Reson.*, **B 105**, 77–82.

Bystrov, V.F. (1976) *Progr. NMR Spectrosc.*, **11**, 41–81.

Case, D.A., (1999) *J. Biomol. NMR*, **15**, 95–102.

Cornilescu, G., Bax, A. and Case, D.A. (2000), *J. Am. Chem. Soc.*, **122**, 2168–2171.

Cornilescu G., Marquardt, J.L., Ottiger, M. and Bax, A. (1998) *J. Am. Chem. Soc.*, **120**, 6836–6837.

Contreras, R.H. and Peralta, J.E. (2000), *Prog. NMR. Spectrosc.*, **37**, 321–425.

Contreras, R.H., Barone, V., Facelli, J. and Peralta J.E. (2003) *Annu. Rep. NMR Spectrosc.*, **51**, 167–260.

Delaglio, F., Torchia, D.A. and Bax, A. (1991) *J. Biomol. NMR*, **1**, 439–446.

Ding, K. and Gronenborn, A. (2004a) *J. Magn. Reson.*, **167**, 253–258.

Ding, K. and Gronenborn, A. (2004b) *J. Am. Chem. Soc.*, **126**, 6232–6233.

Dunning, T.H. (1989) *J. Chem. Phys.*, **90**, 1007–1023.

Edison, A.S., Markley, J.L. and Weinhold, F. (1994a) *J. Biomol. NMR*, **4**, 519–542.

Edison, A.S., Weinhold, F., Westler W.M. and Markley, J.L. (1994b) *J. Biomol. NMR*, **4**, 543–551.

Frisch, M.J., Trucks, G.W., Schlegel, H.B., Scuseria, G.E., Robb, M.A., Cheeseman, J.R., Zakrzewski, V.G., Montgomery Jr. J.A., Stratmann, R.E., Burant, J.C., Dapprich, S., Millam, J.M., Daniels, A.D., Kudin, K.N., Strain, M.C., Farkas, O., Tomasi, J., Barone, V., Cossi, M., Cammi, R., Mennucci, B., Pomelli, C., Adamo, C., Clifford, S., Ochterski, J., Petersson, G.A., Ayala, P.Y., Cui, Q., Morokuma, K., Malick, D.K., Rabuck, A.D., Raghavachari, K., Foresman, J.B., Cioslowski, J., Ortiz, J.V., Baboul, A.G., Stefanov, B.B., Liu, G., Liashenko, A., Piskorz, P., Komaromi, I., Gomperts, R., Martin, R.L., Fox, D. J., Keith, T., Al-Laham, M.A., Peng, C.Y., Nanayakkara, A., Challacombe, M., Gill, P.M.W., Johnson, B., Chen, W., Wong, M.W., Andres, J.L., Gonzalez, C., Head-Gordon, M., Replogle, E.S. and Pople, J.A. (1998) *Gaussian98 Revision A.9.*, Gaussian, Inc., Pittsburgh, PA.

Goddard, T.D. and Kneller, D.G. *SPARKY 3*, University of California, San Francisco.

Harbison, G.S. (1993) *J. Am. Chem. Soc.*, **115**, 3026–3027.

Heikkinen, S., Permi, P. and Kilpeläinen, I. (2001) *J. Magn. Reson.*, **148**, 53–60.

Helgaker, T. and Pecul, M. (2004) Spin–spin coupling constants with HF and DFT methods. In *Quantum Chemical Calculation of Magnetic Resonance Properties. Theory and Applications*, Kaupp, M. Bühl, M. and Malkin, V.G. (Eds.), Wiley-VCH, pp. 101–121.

Helgaker, T., Jensen, H.J.A., Jørgensen, P., Olsen, J., Ruud, K., Ågren, H., Bak, K.L., Bakken, V., Christiansen, O., Coriani, S., Dahle, P., Dalskov, E.K., Enevoldsen, T., Fernandez, B., Hättig, C., Hald, K., Halkier, A., Heiberg, H., Hettema, H., Jonsson, D., Kirpekar, S., Kobayashi, R., Koch, H., Mikkelsen, K.V., Norman, P., Packer, M.J., Pedersen, T.B., Ruden, T.A., Sanchez, A., Saue, T., Sauer, S.P.A., Schimmelpfenning, B., Sylvester-Hvid, K.O., Taylor, P.R. and Vahtras, O. (2001) *DALTON, An ab initio Electronic Structure Program*, release 1.2.

Karplus, M. (1963) *J. Am. Chem. Soc.*, **85**, 2870–2871.

Kay, L.E., Ikura, M., Tshudin, R. and Bax, A. (1990) *J. Magn. Reson.*, **89**, 496–514.
Kay, L.E., Keifer, P. and Saarinen, T. (1992) *J. Am. Chem. Soc.*, **114**, 10663–10665.
Koźmiński, W. and Zhukov, I. (2003) *J. Biomol. NMR*, **26**, 157–166.
Koźmiński, W. and Zhukov, I. (2004) *J. Magn. Reson.*, **171**, 338–344.
Levitt, M.H. (1997) *J. Magn. Reson.*, **126**, 164–182.
Marion, D., Ikura, M., Tschudin, R. and Bax, A. (1989) *J. Magn. Reson.*, **85**, 393–399.
Meissner, A., Duus, J.Ø. and Sørensen, O.W. (1997) *J. Biomol. NMR*, **10**, 89–94.
Ottiger, M., Delaglio, F. and Bax, A. (1997) *J. Magn. Reson.*, **131**, 373–378.
Palmer III, A.G., Cavanagh, J., Wright, P.E. and Rance, M. (1991) *J. Magn. Reson.*, **93**, 151–170.
Pecul, M. and Helgaker, T. (2003) *Int. J. Mol. Sci.*, **4**, 143–157.
Permi, P. and Annila, A. (2000) *J. Biomol. NMR*, **16**, 221–227.
Permi, P., Rosevear, P.R. and Annila, A. (2000) *J. Biomol. NMR*, **17**, 43–54.
Rexroth, A., Schimdt, P., Szalma, S., Geppert, T., Schwalbe, H. and Griesinger, C. (1995) *J. Am. Chem. Soc.*, **117**, 10389–10390.
Sattler, M., Schwedinger, M.G., Schleuchter, J. and Griesinger, C. (1995) *J. Biomol. NMR*, **5**, 11–22.
Schindler, M.M. and Kutzelnigg, W. (1982) *J. Chem. Phys.*, **76**, 1919–1933.
Sitkoff, D. and Case, D.A. (1997) *J. Am. Chem. Soc.*, **119**, 12262–12273.
States, D.J., Haberkorn, R.A. and Ruben, R.J. (1982) *J. Magn. Reson.*, **48**, 286–292.
Stephens, P.J., Devlin, F.J., Chabalowski, C.F. and Frisch, M.J. (1994) *J. Phys. Chem.*, **98**, 11623–11627.
Szyperski, T., Wider, G., Buschweller, J.H. and Wüthrich, K. (1993a) *J. Am. Chem. Soc.*, **115**, 9307–9308.
Szyperski, T., Wider, G., Bushweller, J.H. and Wüthrich, K. (1993b) *J. Biomol. NMR*, **3**, 127–132.
Tjandra, N. and Bax, A. (1997) *Science*, **278**, 1111–1114.
Tolman, J.R., Flanagan, J.M., Kennedy, M.A. and Prestegard, J.H. (1995) *Proc. Natl. Acad. Sci. USA*, **92**, 9279–9283.
Wienk, H.L.J., Martínez, M.M., Yalloway, G.N., Schmidt, J.M., Pérez, C., Rüterjans, H. and Löhr, F. (2003) *J. Biomol. NMR*, **25**, 133–145.
Wirmer, J. and Schwalbe, H. (2002) *J. Biomol. NMR*, **23**, 47–55.